IUCr Crystallographic Computing School

16-21st August 2011 Oviedo (Spain)

Direct Methods Algorithms in Powder Diffraction

Prof. Jordi Rius
Institut de Ciència de Materials de Barcelona, CSIC
Bellaterra, Catalunya (SPAIN)

Solving structures from powder data

Crystal structure solution from powder patterns ⇨ **extraction of integrated intensities** ⇨ **Phases**

Direct Methods

(atomicity)

(positivity)

⇩

Variables are defined in direct space

minimisation by simulated annealing of powder pattern differences

(molecular geometry)

Difficulties:

chemical composition

atomic disorder

data resolution

First remarkable applications of conventional DM to powder data

1/ **Rudolf, Saldariaga-Molina, Clearfield**
J.Phys.Chem. (1986) **90**, 6122-6125.
Synthetic aluminophospate, structure type: ATT, $P2_12_12_1$, CuKα

2/ **McCusker (1988)**
J.Appl.Cryst. (1988) **21**, 305-310.
Sigma-2, a silica clathrasil, structure type: SGT, $I4_1/amd$, λ=1.55Å

3/ **Cernik, Cheetham, Prout, Watkin, Wilkinson, Willis**
J.Appl.Cryst. (1991) **24**, 222-226.
Cimetidine ($C_{10}H_{16}N_6S$), $P2_1/c$, λ=1.46Å

4/ **Oberhagemann, Bayat, Marler, Gies, Rius**
Angew.Chem.Int.Ed.Engl.(1996) 35, 2869.
RUB-15, a layer silicate solved at 2Å resolution, *Iba*2, CuKα_1

Intensities improvement

Intensities are normally extracted either using the **Pawley (1981)** or the **LeBail (1988)** method. Peak overlap can be treated by equi-distributing the multiplet intensity. Other more sophisticated methods are (if applicable):

Squared Patterson function: Estermann, McCusker, Baerlocher (1992) J.Appl.Cryst. 25, 539-543

Anisotropic expansion: Shankland, David, Sivia (1997) J.Mater.Chem. 7, 569-572

Texture: Wessels, Baerlocher, McCusker (1999) Science 284, 477-479

Preferred orientation (statistical check): Altomare, Cascarano, Giacovazzo, Gugliardi (1994) J.Appl.Cryst. 27, 1045-1050.

Some Relevant DM Algorithms for Powder Diffraction (1)

(1995) Rius,Sañé,Miravitlles,Gies,Marler,Oberhagemann *Acta Cryst* A**51** 840-845
SF applied to intensity data at 2Å resolution
(1997) Grosse-Kunstleve,McCusker,Baerlocher *Acta Cryst* A**30** 985-995
FOCUS algorithm incorporating framework information
(1997) Brenner,McCusker,Baerlocher *J.Appl.Cryst.* **30** 1167-1172
Use of envelopes to aid phase determination
(1999) Rius,Miravitlles,Gies,Amigó *J.Appl.Cryst.* **32** 89-87
Proof that SF can be applied to data with systematic overlap
(2000) Rius,Torrelles,Miravitlles,Ochando,Reventós,Amigó *J.Appl.Cryst.* **33** 1208-1211
SF applied to data with accidental overlap (Overlapped E's are updated)
(2002) Altomare,Cuocci,Giacovazzo,Gugliardi,Moliterni,Rizzi *J.Appl.Cryst.* **35** 182-184
DM + Fourier recycling improvements
(2005) Rius-Palleiro,Peral,Margiolaki,Torrelles *J.Appl.Cryst.* **38** 906-911
'Envelope' determination from isomorphous-replacement to fix some phases

Some Relevant DM Algorithms for Powder Diffraction (2)

(2006) Wu,Leineweber,Spence,O'Keefe *Nature* **5** 647-652
CF and E's modification
(2007) Baerlocher,McCusker,Palatinus *Z.Kristallogr.* **222** 47-53
CF and histogram matching
(2007) Rius,Frontera *J.Appl.Cryst.* **40** 1035-1038
SF (in Fourier space) with E's treatment
(2007) Baerlocher,Gramm,Massüger,McCusker,He,Hovmöller,Zou *Science* **315** 1113-16
CF and electron microscopy information
(2008) Altomare,Caliandro,Cuocci,Giacovazzo,Moliterni et al. *J.Appl.Cryst.* **41** 56-61
DM and simulated annealing
(2008) Altomare,Cuocci,Giacovazzo,Kamel,Moliterni,Rizzi *Acta Cryst.* A**64** 326-336
DM and minimally resolution biased electron-density maps
(2011) Rius *Acta Cryst* A**67** 63-67
Patterson SF (in Fourier space) with individual & overlapped I as observed data

DM=conventional direct methods in reciprocal space
SF= direct methods sum function
CF= charge-flipping

The normalised structure factors

$$E^2 = \frac{F^2}{\sum_j f_j^2}$$

Form factor fall-off and thermal vibration decay are removed.
For a crystal structure with *N* equal atoms in the unit cell:

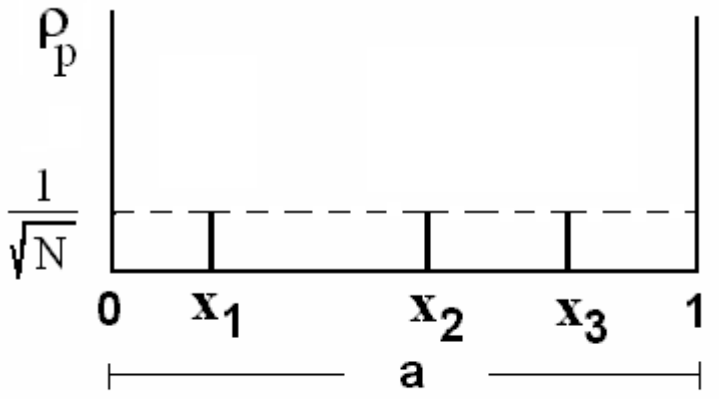

$$\mathbf{E_H} = \frac{1}{\sqrt{N}} \cdot \sum_j e^{i 2\pi \mathbf{H} x_j} = E_{\mathbf{H}} \cdot e^{i\phi_{\mathbf{H}}}$$

The distribution of E's

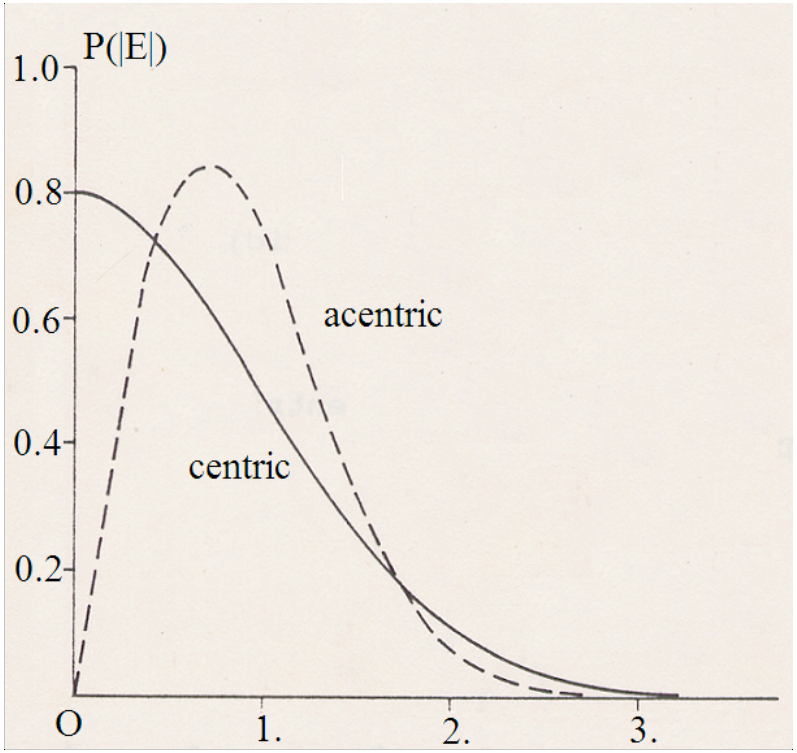

(adapted from D. Viterbo, Direct methods of Solving Crystal Structures pp.58, Ed. By H.Schenk, Plenum Press, New York, 1991)

Wilson (1949) *Acta Cryst.* **2**, 318

$$P_1(E) = \frac{2}{\pi} \cdot E \cdot exp(-E^2)$$

$P_1(E)$ is independent of the structure complexity and holds for any random distribution of atoms in the unit cell. From $P_1(E)$, the theoretical $\langle E^2 \rangle$ and $\langle E \rangle$ values can be derived.

	acentric
$\langle E^2 \rangle$	**1.00**
$\langle E \rangle$	**0.886**

The electron density function

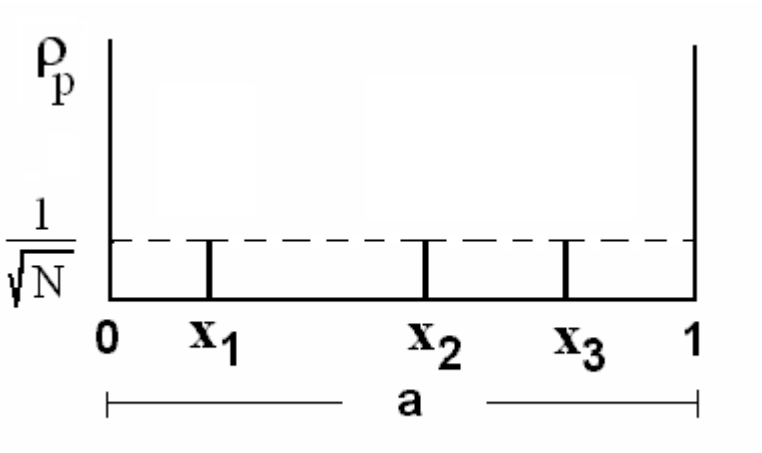

$$\Rightarrow \quad \mathbf{E_H} = \frac{1}{\sqrt{N}} \cdot \sum_j e^{i2\pi \mathbf{H} x_j} = \mathrm{E_H} \cdot e^{i\phi_H}$$

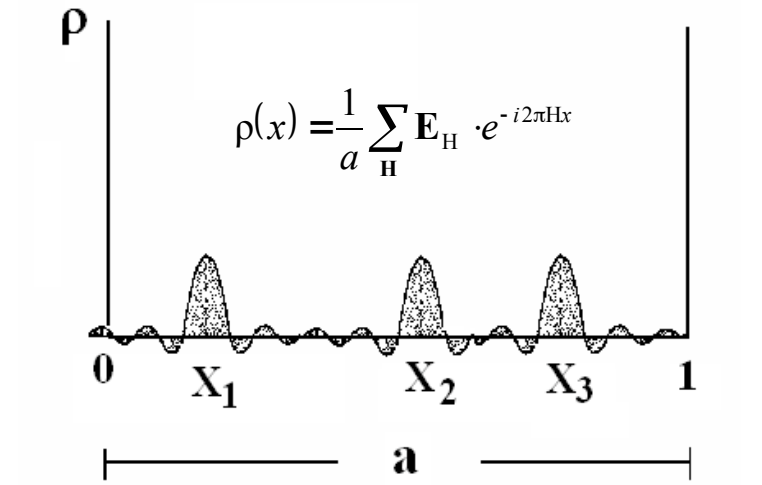

$$\Leftarrow \quad \rho(\mathbf{r}) = \frac{1}{V} \sum_{\mathbf{H}} \mathbf{E_H} \cdot e^{-i2\pi \mathbf{H} \mathbf{r}}$$

(Limited number of Fourier terms)

ATOMIC RESOLUTION !

Data resolution and spreading function

Calculation of ρ with a finite number of Fourier terms (with E's) gives no point atoms. The density distribution is spread.

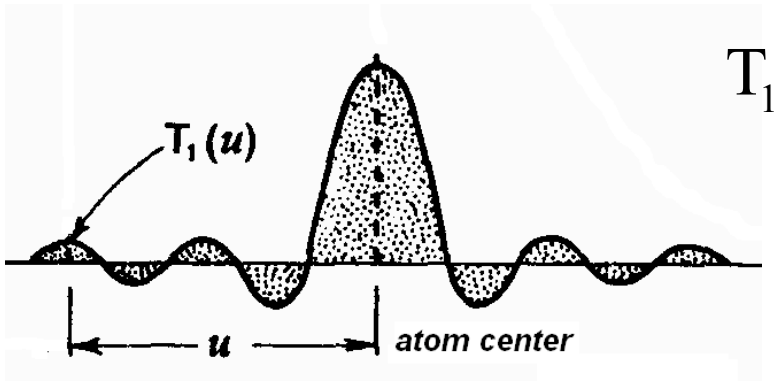

$$T_1(u) = 2 \cdot r^*_{max} \cdot \frac{sin(2\pi r^*_{max} u)}{2\pi r^*_{max} u}$$

(From Lipson & Cochran, 1966)

3D case: 1st zero of $T_3(u)$ at $0.72/r^*_{max}$

Image of the layer silicate RUB-15 at 2 Å resolution

Rius, Sañé,Miravitlles,Gies, Marler, Oberhagemann Acta Cryst. (1995) A51, 840-845.

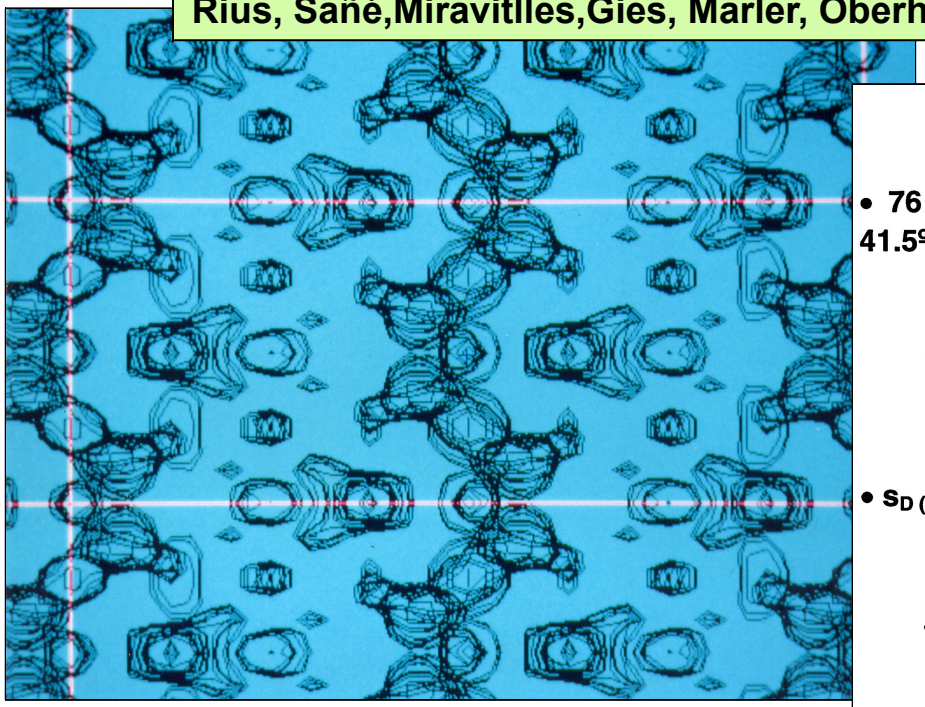

Application of the SUMF-TF

- 76 independent intensities up to $2\vartheta_{max}$ = 41.5º for Cu Kα_1 (almost complete data set)

⇓

2 Angstrons resolution

- $s_{D\,(Si\text{-}Si)} \cong 3.1$ Å ⇒ $d_{min} \cong 2.15$ Å

Parameters introduced in the pha refinement :

- 20 strongest E's ⇒ 65 triplets
- 16 weakest E's ⇒ 98 triplets
- 100 sets refined
- 13 cycles per set
- selection of the solution with the be

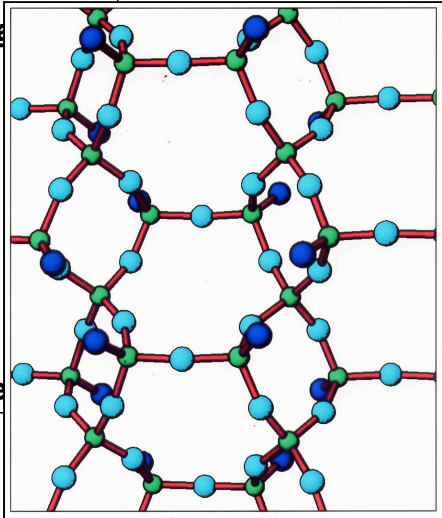

(100) projection of the silicate layer of RUB-15

a= 27.911 *b*=8.408 *c*=11.516 Å

*Iba*2 (*Ibam*)

Institut de Ciència de Materials de Barcelona (J.Rius)

The s.f. of the squared structure

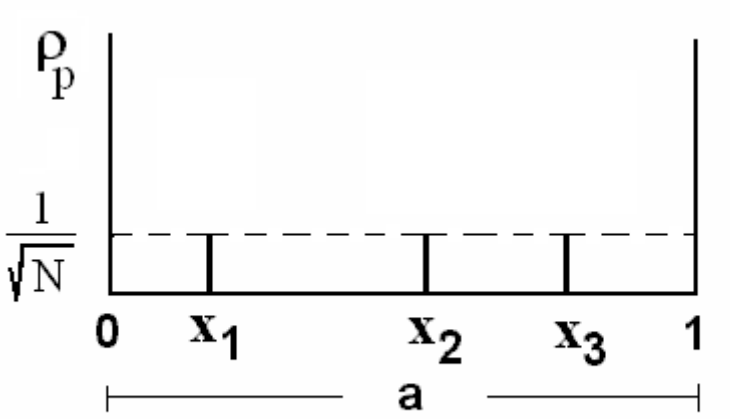

$$\mathbf{E_H} = \frac{1}{\sqrt{N}} \cdot \sum_j e^{i 2\pi \mathbf{H} x_j} = E_{\mathbf{H}} \cdot e^{i\phi_{\mathbf{H}}}$$

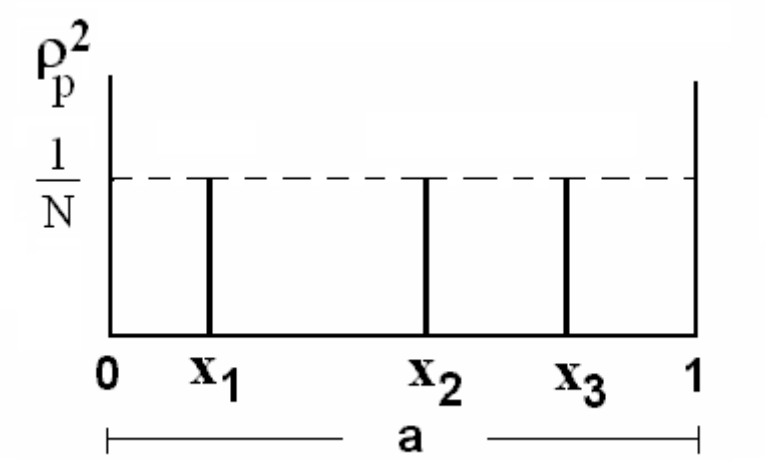

$$\mathbf{G_H} = \frac{1}{N} \cdot \sum_j e^{i 2\pi \mathbf{H} x_j} = G_{\mathbf{H}} \cdot e^{i\psi_{\mathbf{H}}}$$

$$G_{\mathbf{H}} = \frac{E_{\mathbf{H}}}{\sqrt{N}} \qquad \phi_{\mathbf{H}} \approx \psi_{\mathbf{H}}$$

For large H !

The DM origin-free modulus sum function

G is expressed in terms the Φ set of phases.

For any set of G(Φ) fulfilling the atomicity condition, then $\langle G(\Phi)\rangle \approx \langle G(\Phi_{true})\rangle$ so that

$$R_M(\Phi) = \sum_{\mathbf{H}} \left\{ \left(G_{\mathbf{H}} - \langle G \rangle\right) - \left[G_{-\mathbf{H}}(\Phi) - \langle G(\Phi) \rangle \right] \right\}^2 = min!$$

is equivalent to maximising S_M

$$S_M(\Phi) = \frac{2}{\sqrt{N}} \sum_{\mathbf{H}} \left(E_{\mathbf{H}} - \langle E \rangle\right) \cdot G_{-\mathbf{H}}(\Phi) = max!$$

Physical meaning of S_M (I)

$$S_M(\Phi) = \frac{2}{\sqrt{N}} \sum_{\mathbf{H}} \left(E_{\mathbf{H}} - \langle E \rangle\right) \cdot G_{-\mathbf{H}}(\Phi)$$

is the reciprocal space form for

$$S_M(\Phi) \propto \int_V P'_M(\mathbf{u}) \cdot P_M(\mathbf{u}, \Phi) \cdot d\mathbf{u}$$

Physical meaning of S_M (II)

$$S_M(\Phi) \propto \int_V P'_M(\mathbf{u}) \cdot P_M(\mathbf{u}, \Phi) \cdot d\mathbf{u}$$

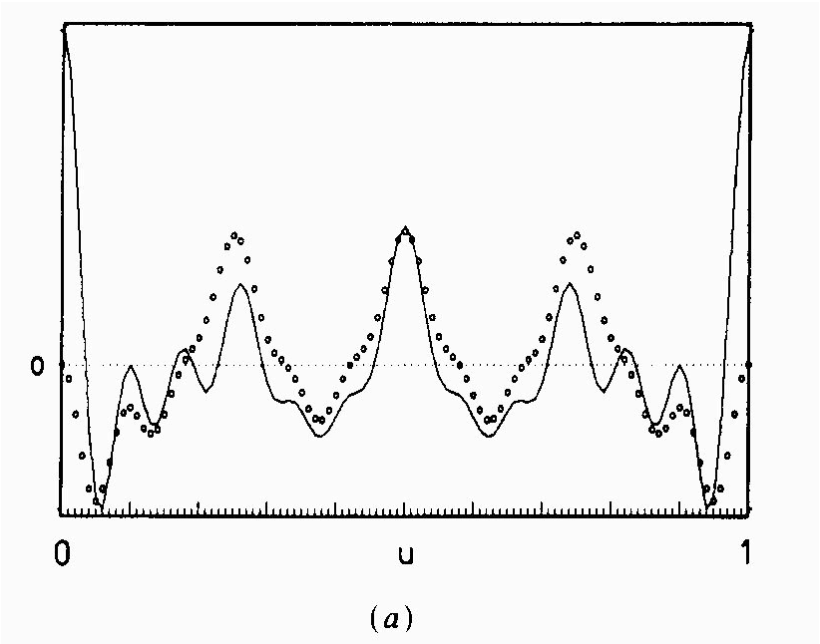

$P_M'(u)$ (dots) and $P_M(u,\Phi)$ (line)

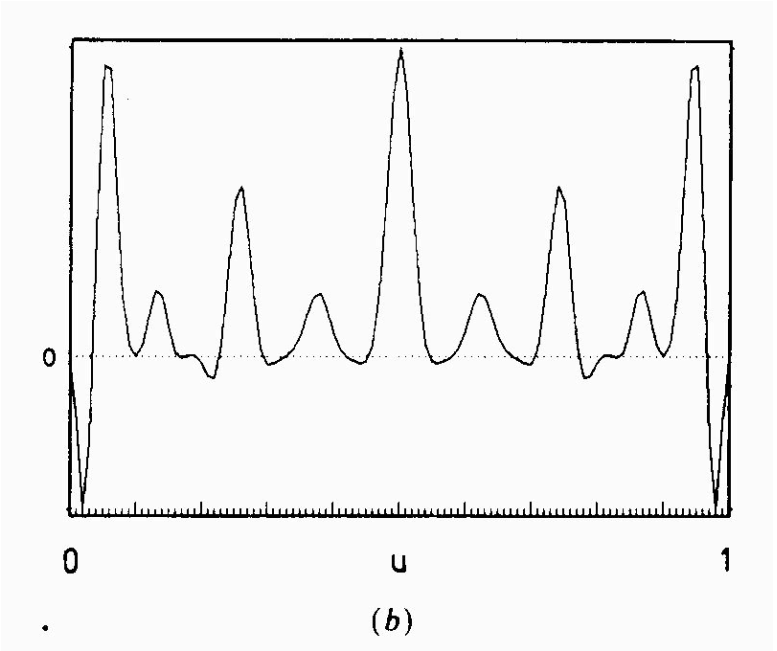

$P_M'(u) \cdot P_M(u,\Phi)$

Institut de Ciència de Materials de Barcelona (J.Rius) 1-D: atoms at 0.0, 0.2, 0.5, 0.75

G_H in terms of $\Phi = \{\ldots, \varphi_h, \ldots\}$

Direct space: $\rho^2(\Phi) = \rho(\Phi) \cdot \rho(\Phi)$ (if atomicity holds)

Reciprocal space:

$$\mathbf{G}_{-\mathbf{H}}(\Phi) = G_{-\mathbf{H}}(\Phi) \cdot e^{i\psi_{-\mathbf{H}}(\Phi)}$$

$$= \frac{1}{V} \sum_{\mathbf{h}} E_{-\mathbf{h}} E_{\mathbf{H}-\mathbf{h}} e^{i(\phi_{-\mathbf{h}} + \phi_{\mathbf{h}-\mathbf{H}})}$$

$$\Downarrow$$

$$G_{-\mathbf{H}}(\Phi) = \frac{1}{V} \sum_{\mathbf{h}} E_{-\mathbf{h}} E_{\mathbf{H}-\mathbf{h}} e^{i(\phi_{-\mathbf{h}} + \phi_{\mathbf{h}-\mathbf{H}} + \psi_{\mathbf{H}})}$$

S_M rearrangement

Expression $S_M=(2/\sqrt{N})\,\Sigma_H(E_H - \langle E\rangle)G_{-H}(\Phi)$ can be rearranged in the form

$$S_M = \frac{2}{\sqrt{N}} \sum_{\mathbf{h}} E_{-\mathbf{h}} e^{i\phi_{-\mathbf{h}}} \left\{ \frac{1}{V} \sum_{\mathbf{H}} \left(E_{\mathbf{H}} - \langle E \rangle\right) \cdot E_{\mathbf{h}-\mathbf{H}} e^{i(\psi_{\mathbf{H}} + \phi_{\mathbf{h}-\mathbf{H}})} \right\} \cong \cong \cong$$

$$\Downarrow$$

$$\{\ldots\} = \text{Fourier coefficient of } \delta_M' = \delta_M \cdot \rho$$

$$\rho = FT^{-1}\left\{ E_{\mathbf{H}} \cdot \exp i\phi_{\mathbf{H}} \right\}$$

$$\delta_M = FT^{-1}\left\{ \left(E_{\mathbf{H}} - \langle E \rangle\right) \cdot exp\, i\psi_{\mathbf{H}} \right\}$$

How to maximise S_M

$$S_M = \frac{2}{\sqrt{N}} \sum_{\mathbf{h}} E_{-\mathbf{h}} e^{i\phi_{-\mathbf{h}}} \left\{ \frac{1}{V} \sum_{\mathbf{H}} \left(E_{\mathbf{H}} - \langle E \rangle \right) \cdot E_{\mathbf{h}-\mathbf{H}} e^{i(\psi_{\mathbf{H}} + \phi_{\mathbf{h}-\mathbf{H}})} \right\} \cong \cong \cong$$

Sequential mode

(S_M-TF refinement using phase relationships, explicitly

$$E_{-\mathbf{h}} \left(E_{\mathbf{H}} - \langle E \rangle \right) E_{\mathbf{h}-\mathbf{H}} \, exp\, i(\phi_{-\mathbf{h}} + \psi_{\mathbf{H}} + \phi_{\mathbf{h}-\mathbf{H}})$$

Rius (1993) *Acta Cryst* A**49**, 406-409

Parallel mode

S-FFT algorithm

Rius et al. (2007) *Acta Cryst* A**63**, 131-134

The S_M-FFT algorithm

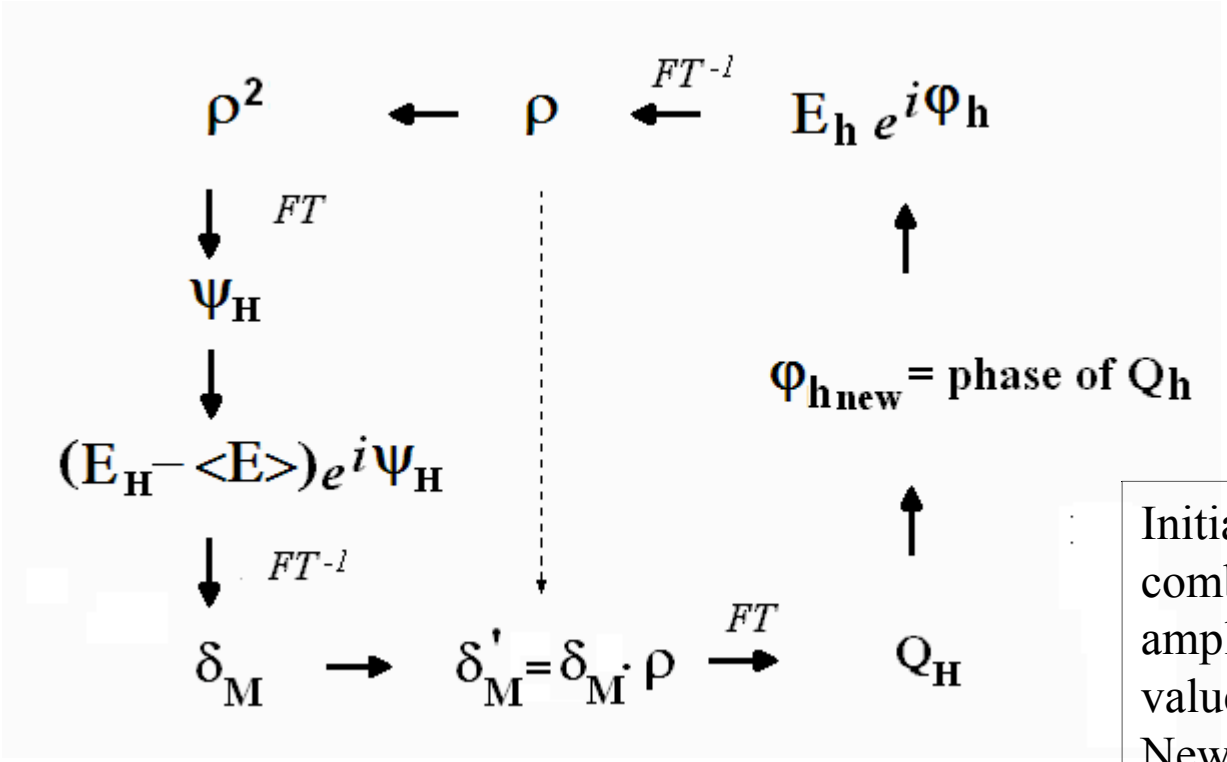

Initial phase values are combined with experimental amplitudes to give initial ρ values (upper right corner). New structure factor estimates Q are obtained by Fourier transforming δ_M'.

Patterson-function direct methods

$$S_M(\Phi) \propto \int_V P_M'(\mathbf{u}) \cdot P_M(\mathbf{u},\Phi)\, d\mathbf{u}$$

Patterson-function DM are based on the existing proportionality between non-origin peaks of modulus and Patterson functions:

$$S_P(\Phi) \propto \int_V P'(\mathbf{u}) \cdot P_M(\mathbf{u},\Phi)\, d\mathbf{u}$$

$$S_P(\Phi) = (2/N)\, \Sigma_{\mathbf{H}} (I_{\mathbf{H}} - \langle I \rangle) \cdot G_{-\mathbf{H}}(\Phi)$$

Rearrangement of S_P

In parallel to S_M, S_P can be rearranged to

$$S_P = \frac{2}{N}\sum_{\mathbf{h}} E_{-\mathbf{h}} e^{i\phi_{-\mathbf{h}}} \left\{ \frac{1}{V}\sum_{\mathbf{H}} \left(I_{\mathbf{H}} - \langle I \rangle\right) \cdot E_{\mathbf{h}-\mathbf{H}} e^{i(\psi_{\mathbf{H}} + \phi_{\mathbf{h}-\mathbf{H}})} \right\} \cong \cong \cong$$

$\Downarrow$

$\{\ldots\}$ is the Fourier coefficient of $\delta_P' = \rho \cdot \delta_P$

$$\rho = FT^{-1}\left\{ w_{\mathbf{H}} \cdot E_{\mathbf{H}} \cdot \exp i\phi_{\mathbf{H}} \right\}$$

$$\delta_P = FT^{-1}\left\{ \left(I_{\mathbf{H}} - \langle I \rangle\right) \cdot exp\, i\psi_{\mathbf{H}} \right\}$$

Powder diffraction intensities

D_i , n_i = global intensity and number of contributing reflections for multiplet i

Intensity of H reflection:

$$I_H = D_i/n_i$$

(all reflections of one multiplet have same I)

Average intensity:

$$\langle I \rangle = (\Sigma_H I_H)/N_H = (\Sigma_i D_i)/N_H$$

Notice that $\langle I \rangle = \langle E^2 \rangle$

S_P-FFT algorithm for Patterson-function DM with powder data

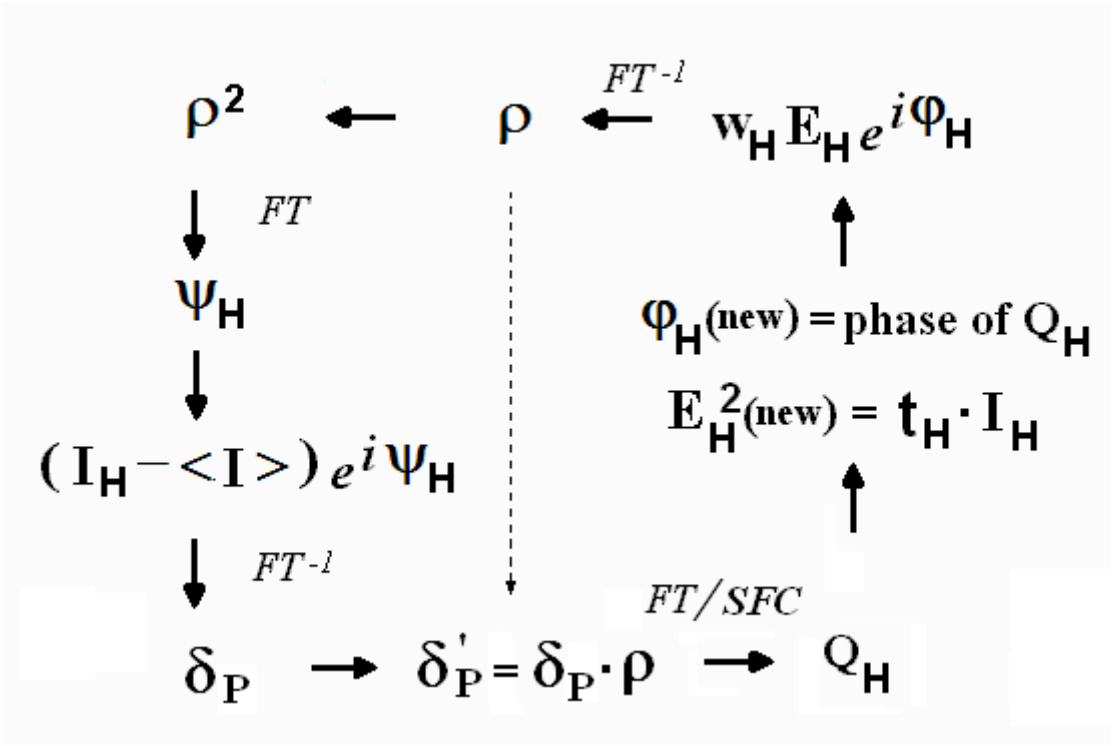

$$E_H^{\,2}(new) = \left(\frac{n_i Q_H^{\,2}}{\sum_k j_{k(i)} Q_{k(i)}^{\,2}} \right) I_H = t_H I_H$$

Initial phase values are combined with experimental and extrapolated amplitudes to give initial ρ values (upper right corner). The measured multiplet intensities are introduced via the (I_H - <I>) coefficients. New structure factor estimates are obtained either by Fourier tranforming δ_P' or directly from the N top-ranked Fourier peaks (*SFC*) of δ_P' . For overlapped reflections, E_H^2 values are updated every cycle while keeping the global intensity of each multiplet constant.

Institut de Ciència de Materials de Barcelona (J.Rius)

INORGANIC V.S. ORGANIC COMPOUNDS IN POWDER DIFFRACTION

Reasons for the success in solving crystal structures from inorganic compounds (IC) compared to molecular ones:

1) IC tend to have smaller unit cells or higher metrics (less accidental peak overlap);

2) IC possess longer bond distances (less data resolution requirements);

3) IC contain stronger scatterers with higher contrast (smaller effective number of atoms);

4) IC are more stable (consistency of the measured data set over the whole 2-theta range).

Aerinite blue

a= 16.882 *c*= 5.225Å, ***P3c1***

250 integrated intensities mostly affected by systematic overlap

(LURE DW22, capillar 1mm)

d_{min}: 1.3-1.2 Å

E map

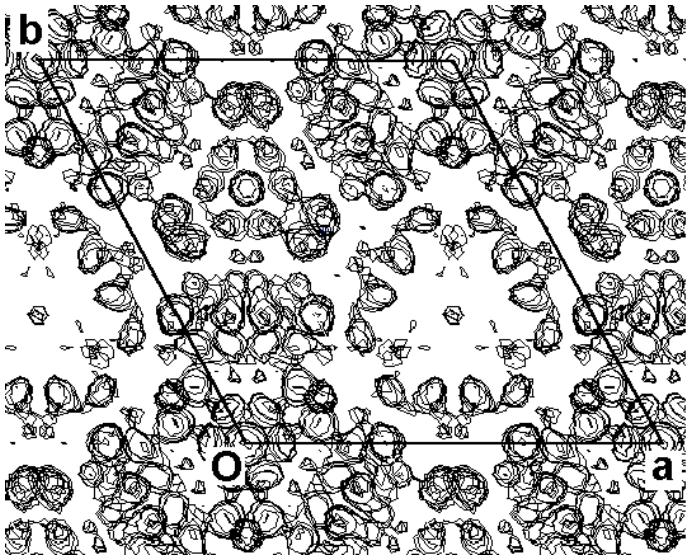

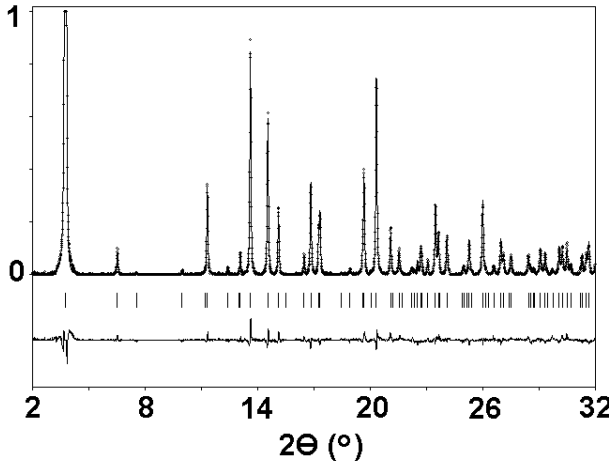

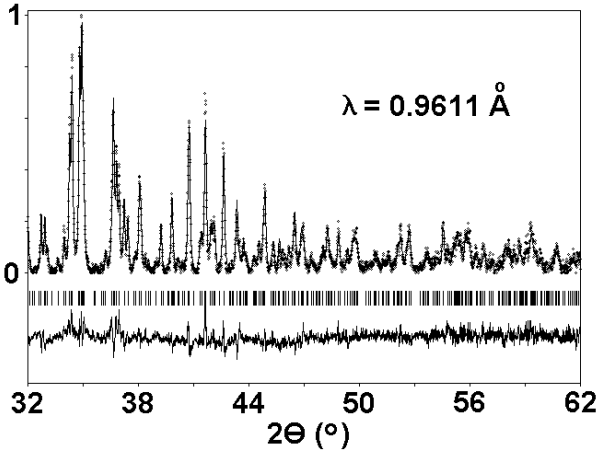

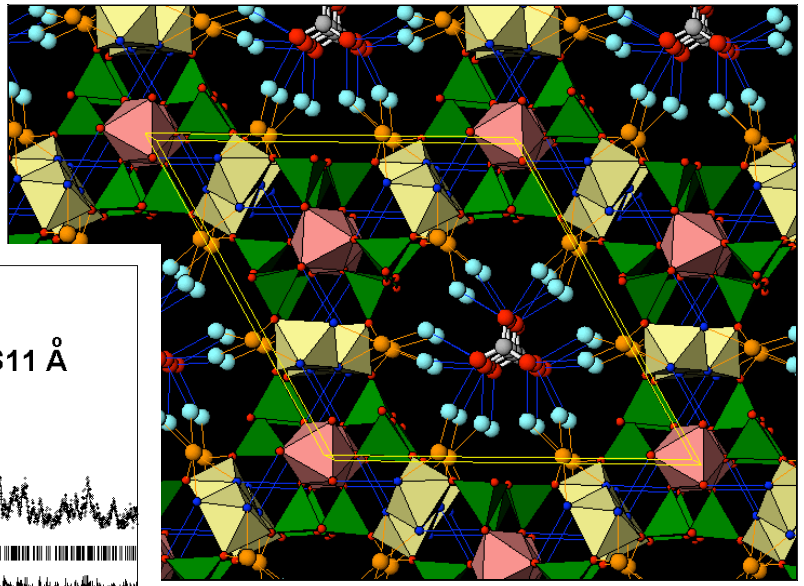

Rius,Elkaim,Torrelles (2004)
Eur.J. Mineral. 16, 127

Institut de Ciència de Materials de Barcelona (J.Rius)

Sanjuanite

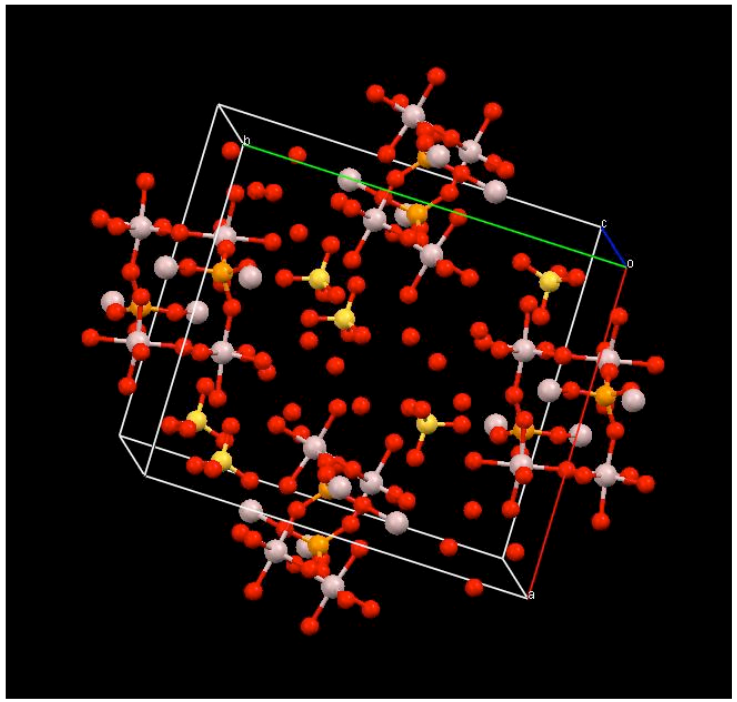

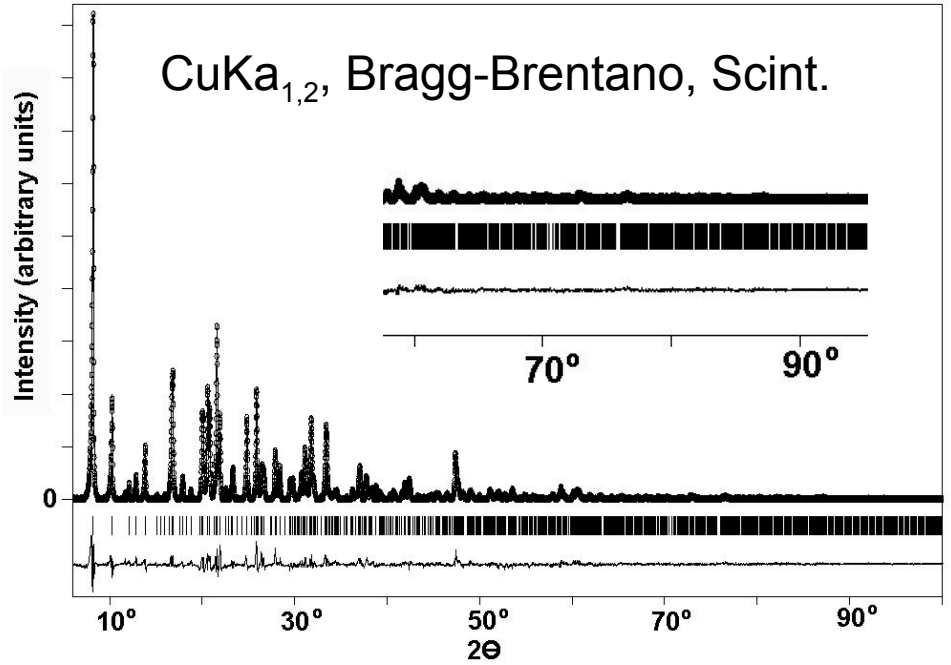

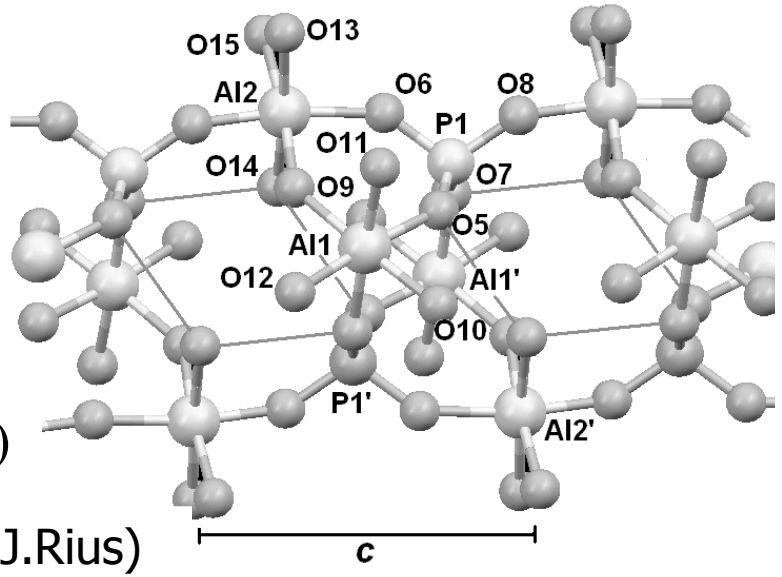

$Al_2(PO_4)(SO_4)(OH)\cdot 9H_2O$, Z= 4,
Space group $P2_1/n$, V = 1451Å^3
a=13.92, b=17.24, c=6.11Å, β=98.3º

The Canadian Mineralogist, **49**, 835 (2011)

Institut de Ciència de Materials de Barcelona (J.Rius)

TABLE 1. SUMMARY OF RELEVANT INFORMATION FOR THE RIETVELD REFINEMENT OF SANJUANITE

Unit-cell parameters	
a, *b*, *c*	13.9163(5), 17.2422(5), 6.1125(3) Å
β	98.255(4)°
Unit-cell volume, *Z*	1450.7(5) Å³, 4
Space group	$P2_1/n$ (#14)
Radiation, wavelength	Cu$K\alpha_{1,2}$, 1.54059, 1.54443 Å
2θ range	5.995 -100.000°
Number of data points	6268
Peak range in FWHM	20
Number of contributing reflections	1440
Number of profile parameters	10
Number of structural parameters	68
Number of structural restraints	27
Profile function	pseudo-Voigt
Peak breadth	0.13° at 2θ =20°, 0.09° at 2θ = 85°
March–Dollase coefficient	1.20(2)
Preferred orientation direction	[$\bar{2}$ 0 3]
Zero shift	–0.0661(5)°
Background estimation	see Experimental
R_{wp}, χ^2	0.097*, 2.47
Weighting scheme	$1/y_o$

TABLE 2. FINAL REFINED COORDINATES OF ATOMS IN SANJUANITE

Atom	*x/a*	*y/b*	*z/c*	Occupancy
S1	0.1264(5)	0.3459(4)	0.4154(16)	1
P1	0.1212(7)	0.0463(6)	0.6855(26)	1
Al1	-0.1099(7)	0.1155(6)	0.5944(22)	1
Al2	0.1809(8)	0.0688(7)	1.2090(25)	1
O1	0.0730(10)	0.3868(8)	0.5733(23)	1
O2	0.1157(10)	0.3795(9)	0.1902(22)	1
O3	0.2312(6)	0.3494(9)	0.5123(30)	1
O4	0.0968(11)	0.2635(5)	0.3956(32)	1
O5	0.1090(13)	-0.0425(8)	0.6397(28)	1
O6	0.1781(13)	0.0826(10)	0.5138(28)	1
O7	0.0276(8)	0.1010(11)	0.6646(40)	1
O8	0.1748(13)	0.0547(12)	0.9249(32)	1
O9	-0.1507(13)	0.0399(8)	0.7903(32)	1
O10	-0.0790(13)	0.1981(10)	0.4080(31)	1
O11	-0.2432(7)	0.1385(11)	0.4860(31)	1
O12	-0.1104(12)	0.1930(10)	0.8185(27)	1
O13	0.3208(9)	0.0524(11)	1.2296(40)	1
O14	0.0469(11)	0.0993(10)	1.1403(40)	1
O15	0.2149(13)	0.1798(9)	1.1860(45)	1
O16	-0.0173(11)	0.3300(9)	0.8685(37)	1.25*
O17	-0.1028(12)	0.4512(9)	0.2361(38)	1.25*
O18	0.3053(11)	0.1940(11)	0.8001(39)	1.25*

TABLE 3. APPROXIMATE BALANCE OF BOND VALENCES (*vu*) FOR SANJUANITE

Atom (*X*)	S1	P1	Al1	Al2	Σ_C v	Probable H bonds				O··*X*··O (°)
O1	**1.50**				**1.50**	← **O16**	← **O17**			
	1.48					2.7	3.0			
O2	**1.50**				**1.50**	← **O11**	← **O16**	← **O13**		
	1.48					2.5	2.6	3.1		
O3	**1.50**				**1.50**	← **O12**	← **O11**			
	1.50					2.7	2.8			
O4	**1.50**				**1.50**	← **O10**	← **O15**			
	1.48					2.7	2.7			
O5		**1.25**	**0.50**		**1.75**	← **O14**				
		1.56	1.91			2.9				
O6		**1.25**		**0.52**	**1.77**	← **O18**				
		1.54		1.88		3.0				
O7		**1.25**	**0.50**		**1.75**	← **O14**				
		1.60	1.92			2.9				
O8		**1.25**		**0.74**	**1.99**	-				
		1.55		1.74						
O9(H)			**0.50**	**0.46**	**0.96**	-				
			1.91	1.92						
O10(w)			**0.50**		**0.50**	→ **O18**	→ **O4**			
			1.91			2.5	2.7			104
O11(w)			**0.50**		**0.50**	→ **O2**	→ **O3**			
			1.92			2.5	2.9			121
O12(w)			**0.50**		**0.50**	→ **O3**	→ **O16**			
			1.91			2.7	2.7			126
O13(w)				**0.43**	**0.43**	→ **O2**	→ **O16**			
				1.95		3.1	3.1			114
O14(w)				**0.45**	**0.45**	→ **O5**	→ **O7**			
				1.93		2.9	2.9			120
O15(w)				**0.40**	**0.40**	→ **O4**	→ **O18**			
				1.98		2.7	2.8			137
O16(w)					**0.00**	← **O12**	← **O13**	→ **O1**	→ **O2**	
						2.7	3.1	2.7	2.6	108
O17(w)					**0.00**	← **O18**	→ **O1**			
						2.9	3.0			142
O18(w)					**0.00**	← **O10**	← **O15**	→ **O6**	→ **O17**	
						2.5	2.8	3.0	2.9	108
Σ_A v	6	5	3	3						

Owing to the expected regularity of their coordination polyhedra and to the large uncertainty in the cation–O distances (s.u.s ≈ 0.02 Å), ideal bond-valences v_i (upper value in bold) are assumed for S1, P1 and Al1; for Al2, they are estimated from the individual Al–O distances d_i (lower value in Å), with expression $v_i = K_{Al}\, d_i \exp(-p_{Al} d_i)$, where $p_{Al} = 3.13$ is taken from Rius & Plana (1982) and Allmann (1975), and $K_{Al} = 98.6$ is fitted to the individual coordination polyhedron to satisfy the charge of Al^{3+}. Owing to the low accuracy of the O…O distances (s.u.s ≈ 0.1 Å), only the donor (→) or acceptor (←) character of each probable H bond is given. In the last column, the value of the O…*X*…O angle (°) is listed (except for O16 and O18 in a tetrahedral environment, where it corresponds to the average of the six O…*X*…O angles).

Application of DM to organic compounds

DM can cope with molecular compounds, only if intensity data reach **1.1-1.2 Å** resolution. This is the high angle portion of powder patterns where

1. peak overlap is most severe,

2. intensity statistics poorer and

3. any inconsistency in the data set (e.g. the variation in unit cell dimensions or radiation damage during data acquisition) is most critical.

Part of these limitations can be experimentally overcome with a fast read-out solid-state microstrip detector.

Treatment of peak overlap

The phasing algorithm must be also **capable of handling the very severe peak overlap** of the high-angle region. Patterson-function direct methods[2] is a promising solution for automated solution of molecular compounds.

All calculations have been carried out with XLENS_PD6 (available at www.icmab.es/xlens).

[1]Rius, J.; Frontera, C., *J. Appl. Cryst.* **2007**, 40, 1035-1038.
[2]Rius,J. (2011) *Acta Cryst* A**67**, 63-67.

Example 1

Triphenylphosphine

$C_{18}H_{15}P$

$P2_1/c$

V = 1460 Å^3

1) As-received from Aldrich

2) Recrystallised from hot acetone (by Norberto Masciocchi)

Boths sets measured by Fabia Gozzo at SLS (Mythen-II detector)

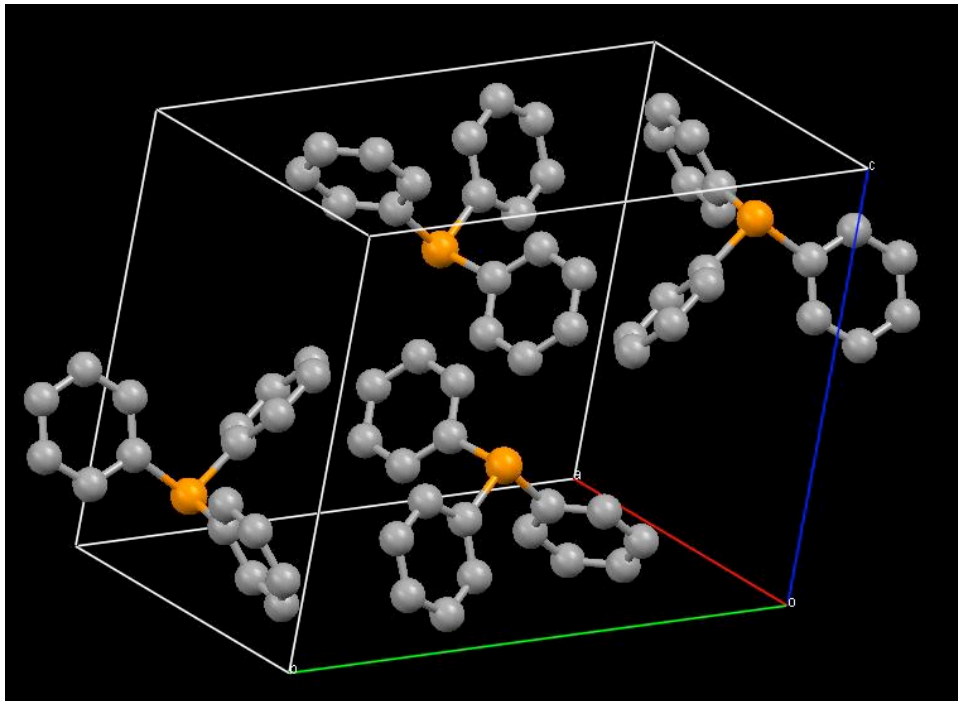

Institut de Ciència de Materials de Barcelona (J.Rius)

d	FWHM
>5	<0.019
2.5	0.027
1.5	0.040
1.1	0.053
1.0	0.059

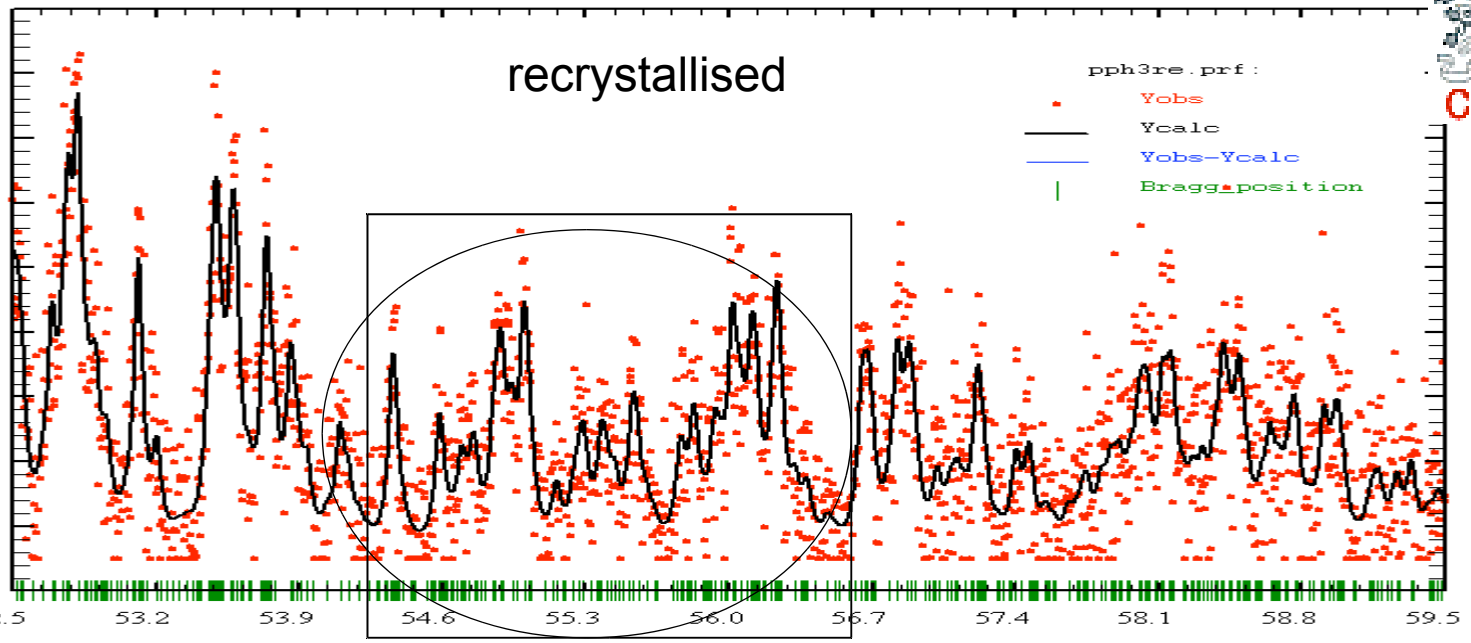

d	FWHM
>5	<0.023
2.5	0.035
1.5	0.050
1.1	0.067
1.0	0.075
t =0.5	
25 x FWHM	

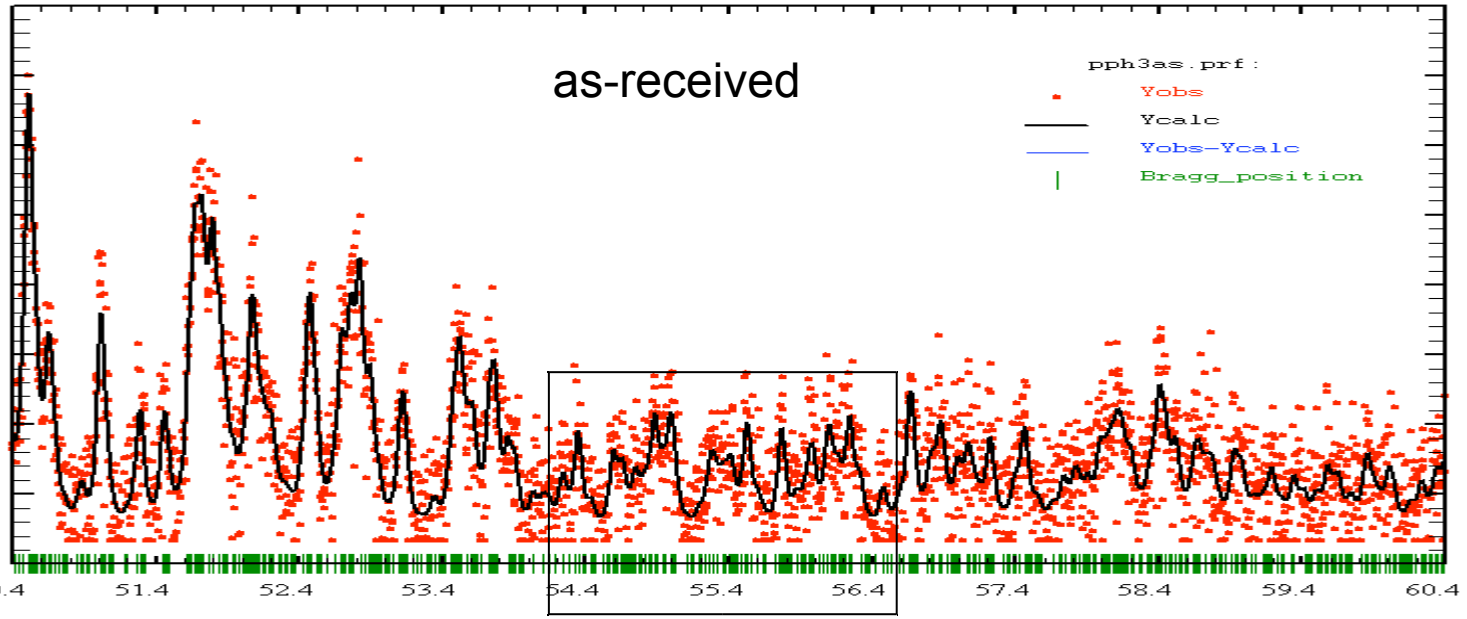

XLENS_PD6 applied to powder data of the recrystallized sample developed the complete model with accurate positions. For the 'as received' sample, the XLENS result is shown below:

d_{min}= 1.10Å

B_{over}= 4.7 Å^2

Success rate= 10 / 50

CC_{true}: 0.86-0.84

CC_{wrong}: <0.825

N. strong refl.= 320

N. refl. (E > 1.15) = 825

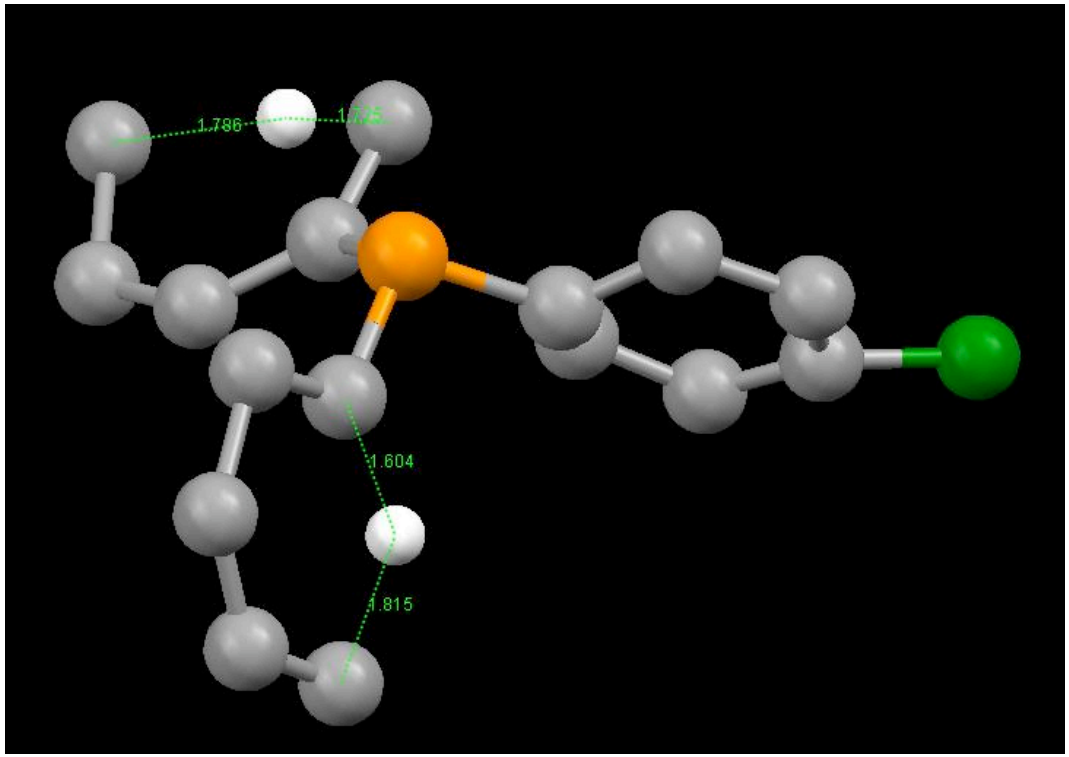

Institut de Ciència de Materials de Barcelona (J.Rius)

Example 2

Structure of (S)-(+)-Ibuprofen from powder data

Relevant information:

Chemical name: 2-[4-(2-methylpropyl)phenyl] propanoic acid

Formula of cyclic hydrogen-bonded dimer: C_{26} H_{16} O_4, *Z*=2

Space group: *P*2_1

Volume: 1246 Å^3

Data measured with MYTHEN-II by F. Gozzo (SLS)

A.FREER*,J.BUNYAN, N.SHANKLAND AND D. SHEEN. *Acta Cryst.* (1993). C49, 1378-1380

d	FWHM
>10Å	0.014º
2.5	0.023
1.5	0.031
1.1	0.040

0.5 x FWHM

25 x FWHM

Cauchy prof.

1.00097 Å

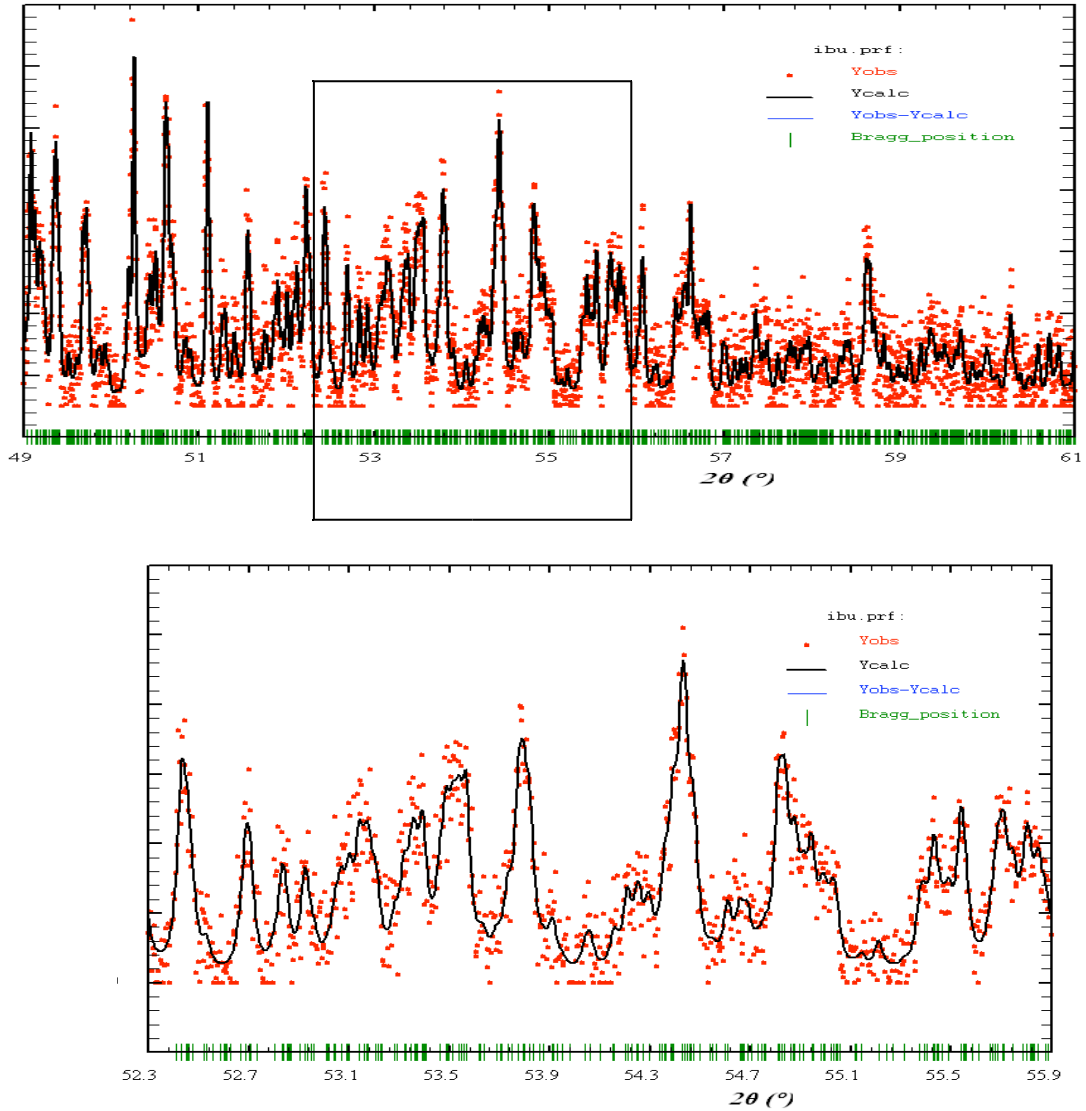

Institut de Ciència de Materials de Barcelona (J.Rius)

Summary of DM with XLENS:

d_{min}= 1.10Å B_{over}= 5.2 Å^2

Success rate= 7 / 25

CC_{true}: 0.92-0.89

CC_{wrong}: <0.85

N. strong refl.: 284

N. refl. with E's > 1.15= 795

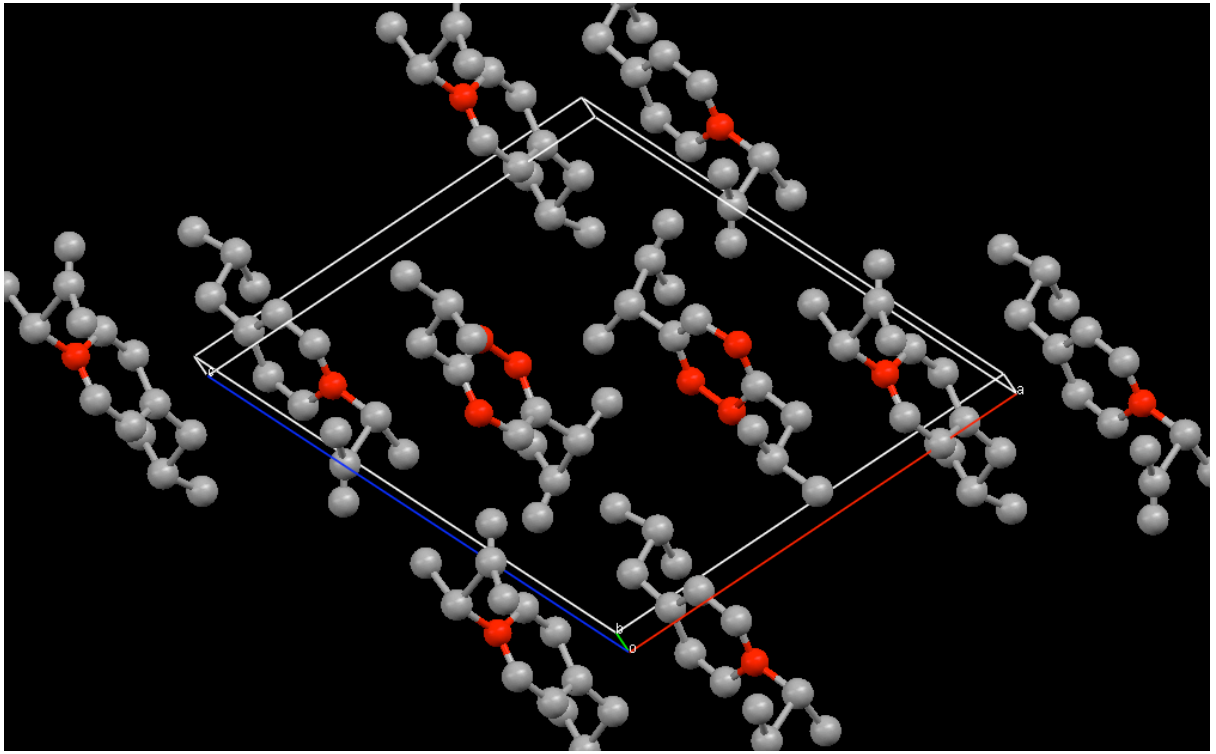

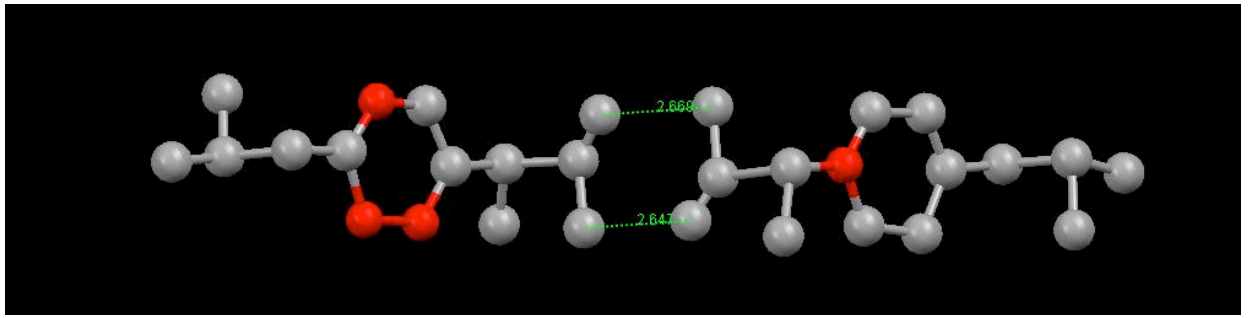

Institut de Ciència de Materials de Barcelona (J.Rius)

Intramolecular distances directly from DM from powder data

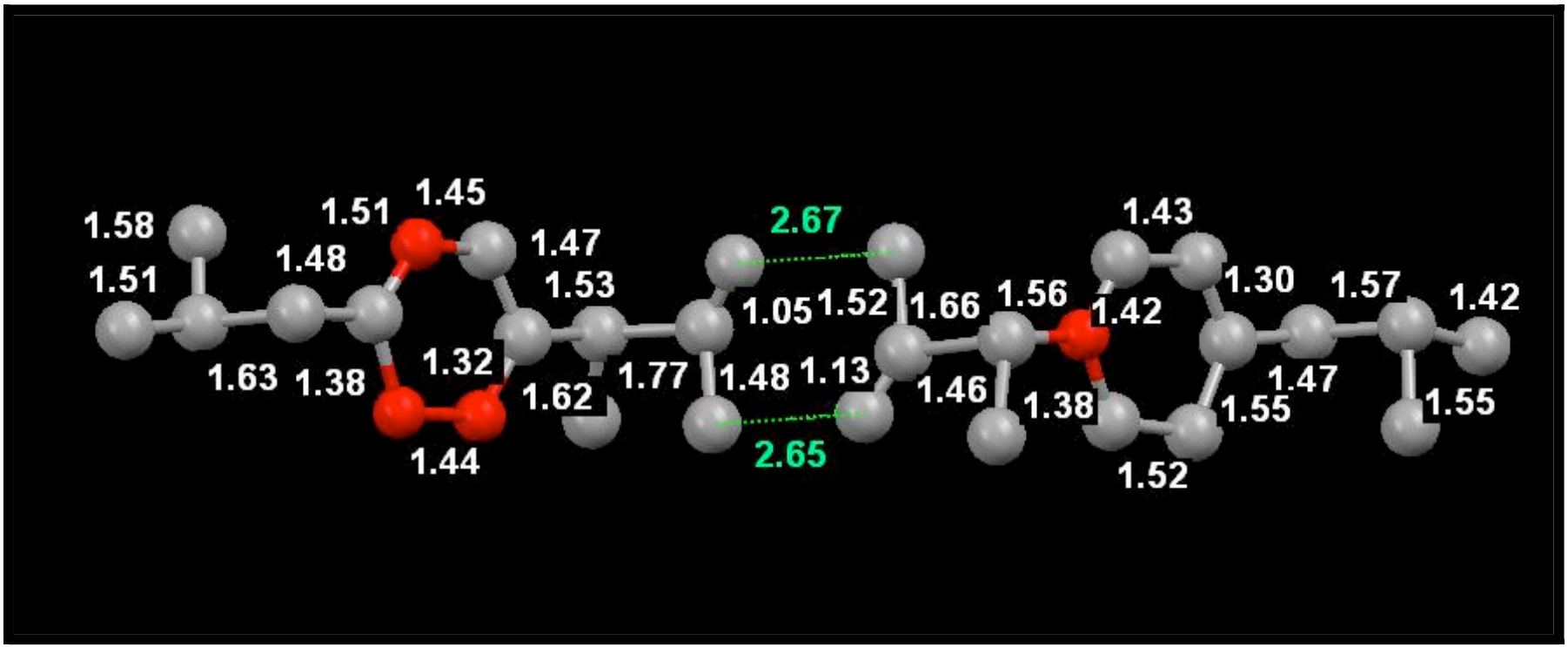

Rius,J. (2011) *Acta Cryst* A**67**, 63-67

Calcium hydroxyphosphonoacetate

R.M.P. Colodrero et al. (2011) Cryst. Growth Des. 11, 1713-22

$Ca_5(O_3PCHOHCOO)_2(HO_3PCHOHCOO)_2 \cdot 6H_2O$

a=29.72 b=8.845 c=11.31 Å β=93.24º

V=2969 Å^3 , $I2/a$, Z=4

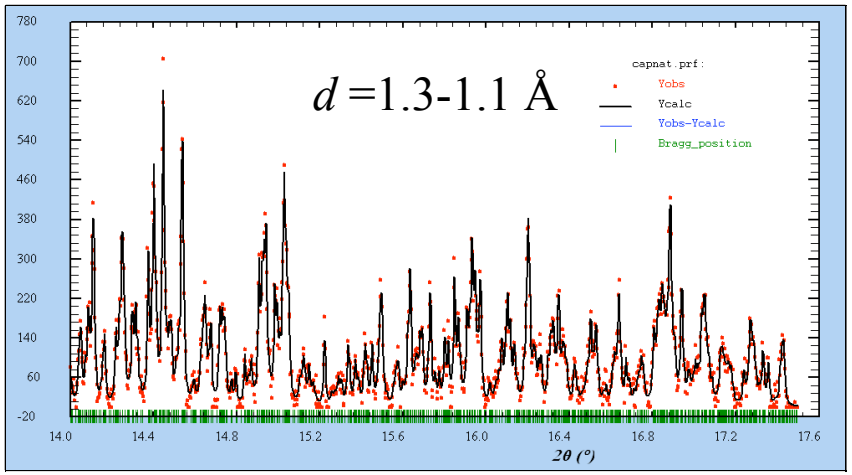

Experimental:

ID31 (ESRF)

λ=0.30

2θ from 1.5 to 20º

Δ=0.003º capillary

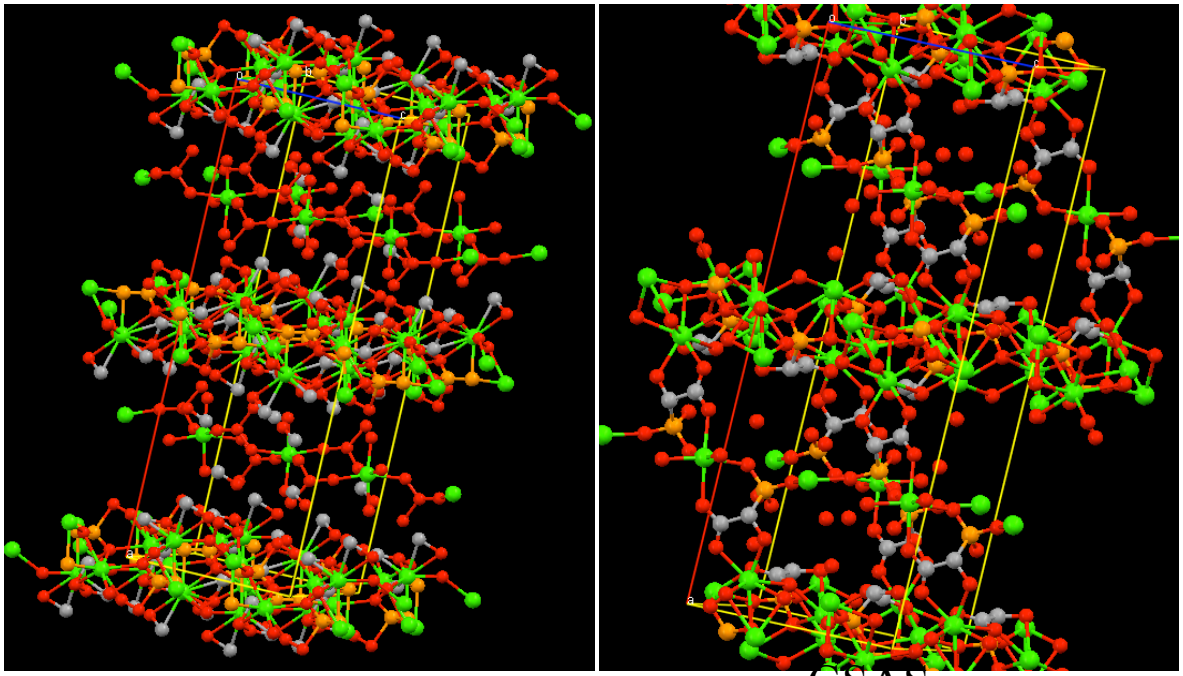

XLENS®_PD6

GSAS

Institut de Ciència de Materials de Barcelona (J.Rius)

Open-Framework Nickel Succinate, $[Ni_7(C_4H_4O_4)_6(OH)_2(H_2O)_2]\cdot 2H_2O$: A New Hybrid Material with Three-Dimensional Ni–O–Ni Connectivity**

Paul M. Forster and Anthony K. Cheetham*

Angew. Chem. Int. Ed. 2002, *41*, No. 3

a= 21.0286 c=45.7728 Å *R*-3*c* *Z*=18

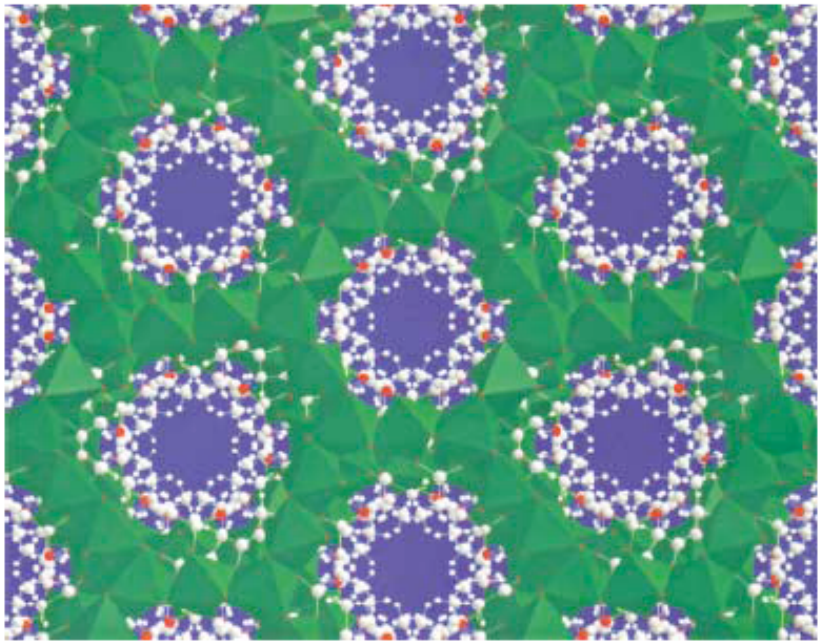

Figure 1. View of the nickel succinate structure down the *c* axis.

(from single crystal data)

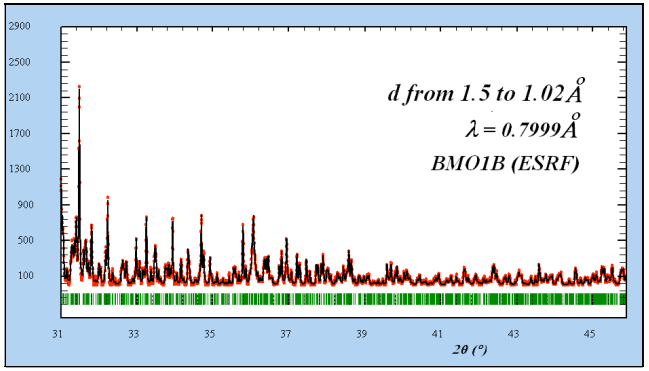

K3 powder data kindly supplied by
Dr. Nathalie Guillou
Inst. Lavoisier-Franklin
Univ. de Versailles (France)

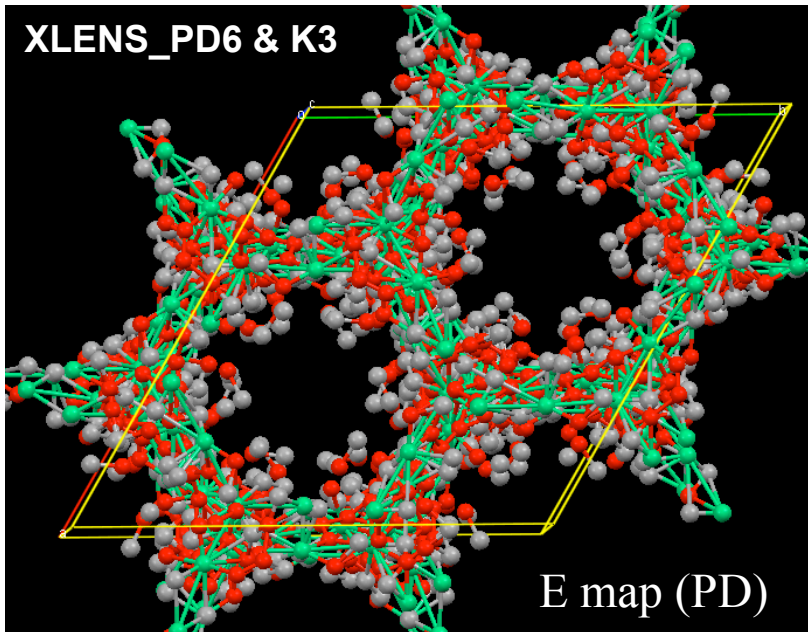

Institut de Ciència de Materials de Barcelona (J.Rius)

Patterns with systematic overlap

limited accidental peak overlap ↔ high effective data resolution

(if systematic peak overlap can be treated)

space groups affected by systematic overlap (%):	
• **with cubic lattice:**	**33%**
• **with tetragonal lattice:**	**21%**
• **with hexagonal lattice:**	**65%**

DM with systematic overlap

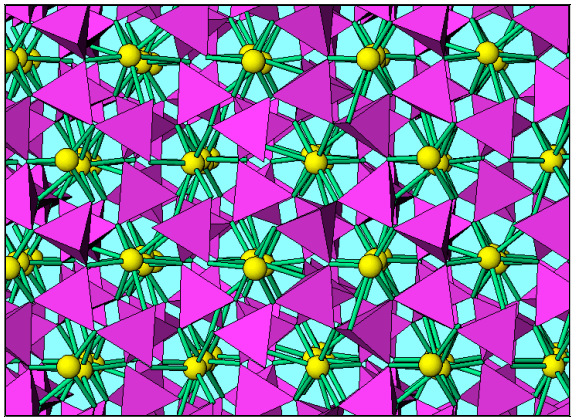

M.Dougill, Nature (1957) 180, 192

Main phase in High Alumina Cement:
$CaAl_2O_4$ (filled trydimite structure type)

⇩

hydraulic reaction (T<20ºC)

⇩

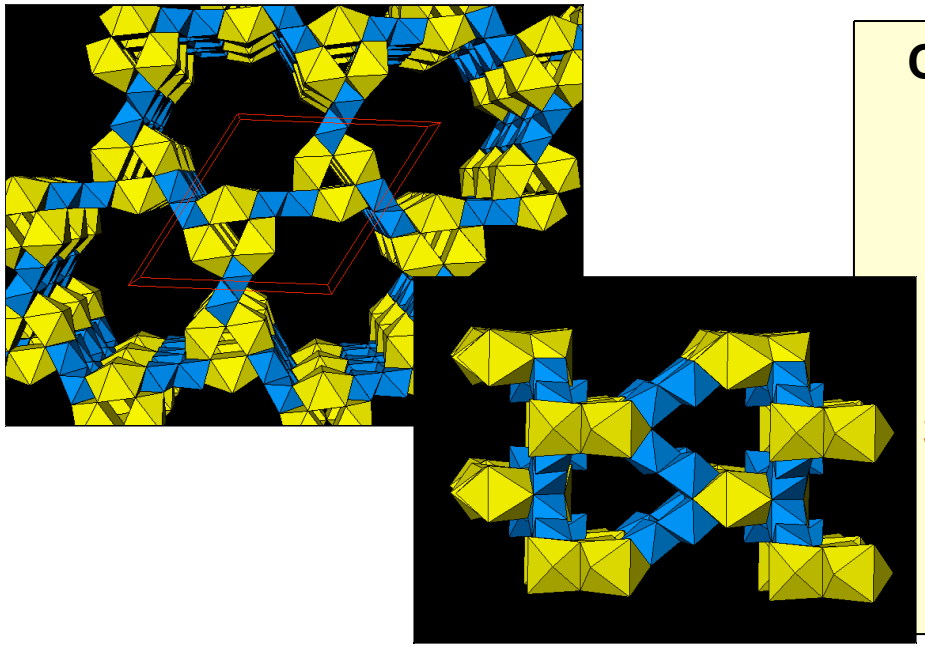

CAH_{10} (gives strength to set cement) + amorphous content

$CaAl_2(OH)_8(H_2O) \cdot 1.84H_2O$
***a* = 16.387 *c* = 8.279Å *V* = 1925Å^3**
***P*6$_3$/*m* *Z*=6 ρ_{calc}=1.55g/cm3**
30 resolved + 128 syst. overlapped (Lab. data)

***Angew. Chem. Int. Ed.* (1998) 37 72**

Institut de Ciència de Materials de Barcelona (J.Rius)